Coral Reefs (2022) 41:369–382
https://doi.org/10.1007/s00338-022-02238-7

REPORT

Investigating the ability of coral reefs to protect shorelines in the Republic of Kiribati

Heather E. Summers[1] · **Simon D. Donner**[1]

Received: 17 July 2021 / Accepted: 7 March 2022 / Published online: 31 March 2022

Abstract The three-dimensional (3D) structure of living coral communities provides frictional resistance to waves and currents. Coral bleaching events can lead to a shift in coral assemblages toward stress-tolerant colonies, potentially reducing reef structural complexity and, in turn, wave attenuation. This is a particular concern in low-lying coastal regions at risk from sea-level rise. In this study, we examined trade-offs between reef resilience and reef structural complexity (defined into three distinct variables, i.e., surface rugosity, standard deviation of elevation, and terrain ruggedness) in Kiribati's Tarawa and Abaiang Atolls, which are subject to frequent El Niño-driven heat stress. Analysis of benthic cover data and 3D reconstructions of the fore reefs indicate that structural complexity increases with coral cover, rather than coral diversity, although the relationship depends on the metric used and on the morphology of the dominant coral species. Contrary to expectations, surface rugosity and standard deviation of elevation were not significantly different between the bleaching-resistant reefs of South Tarawa, dominated by the encrusting species *Porites rus*, and the more diverse sites in Abaiang and North Tarawa; terrain ruggedness was significantly greater at South Tarawa sites. A wave attenuation model, however, suggested that wave energy may nonetheless be higher in South Tarawa due to years of local mining of reef rock from the reef flat. Taken together, the results suggest that the survival of stress-tolerant corals could mitigate against losses of structural complexity from repeated bleaching events. These findings illustrate the need for more research bridging ecology and geology to establish how wave attenuation is altered by climate-driven regime shifts on coral reefs.

Keywords Structure-from-motion photogrammetry · Reef morphology · Shoreline protection · Structural complexity · Coral reef ecology · *Porites rus*

Introduction

Coral reefs protect shorelines and can reduce up to 97% of offshore wave energy (Ferrario et al. 2014). Shoreline protection is critical for low-lying atolls and reef islands that are vulnerable to the impacts of rising sea-level and high wave events (Storlazzi et al. 2018; Costa et al. 2019). The interaction between sea-level, waves, and reef properties such as topography, bottom roughness, and size governs nearshore hydrodynamics on atolls and together influences the extent to which islands are impacted by the sea (Kench and Brander 2006; Quataert et al. 2015). In general, wider reef flats with a lower water depth better dissipate offshore wave energy through bed friction compared to narrow reef flats with a higher water depth (Kench and Brander 2006). Additionally, a greater bottom roughness on the reef flat results in decreased wave runup because surface roughness creates frictional drag as the waves and currents pass over the reef.

The relative importance of bottom friction on the reef flat depends on the fore reef slope and complexity. For coral reefs with a steep slope, bottom friction on the reef flat is negligible as a means of dissipating wave energy compared to turbulence, while the opposite is true for

Topic Editor Lauren T. Toth

✉ Simon D. Donner
simon.donner@ubc.ca

[1] Department of Geography, University of British Columbia, Vancouver, BC V6T 1Z2, Canada

relatively flat reefs (Gourlay and Colleter 2005; Quataert et al. 2015). The role of fore reef structural complexity on the reef in wave attenuation is less clear; Quataert et al. (2015) reported that increased fore reef friction generates higher wave-induced setup and thus results in greater wave runup, whereas Monismith et al. (2015) found that reefs with high geometric complexity provide greater shoreline protection.

It is generally well accepted that the effectiveness of wave energy dissipation by coral reefs is likely to diminish under projected climate change scenarios (Sheppard et al. 2005; Monismith et al. 2015; Quataert et al. 2015). An increase in the frequency and intensity of coral bleaching, in combination with the effects of ocean acidification and local human disturbance, can reduce reef structural complexity, reef integrity, and reef accretion by reducing the extent, diversity, and growth rate of living corals (Harris et al. 2018; Perry et al. 2018; Cornwall et al. 2021). For example, coral loss from anomalous sea surface temperatures (SST) and mass bleaching events have led to declines in rugosity (Couch et al. 2017; Magel et al. 2019), coral skeletal integrity (Leggat et al. 2019), and reef carbonate production (Lange and Perry 2019; Courtney et al. 2020). In addition, sea-level rise is expected to raise mean water depths across a reef thereby allowing higher wave energy to propagate onto reef surfaces resulting in decreased shoreline protection (Sheppard et al. 2005). Sea-level rise combined with slow or nonexistent coral growth due to bleaching, acidification, and other stressors may lead to "drowned" reefs where reef growth fails to keep pace with rising sea level (Perry et al. 2018; Cornwall et al. 2021). Net accretion of reefs cease when rates of erosion exceed the rates of growth and recruitment, resulting in decreased capacity to attenuate offshore wave energy (Principe et al. 2012).

A challenge in studying the effects of climate change on coral reef ability to attenuate waves is that reefs are highly dynamic and heterogeneous systems composed of varying coral species and morphologies (Graham and Nash 2013). Predicting the impact of reduced coral structural complexity and biodiversity on coastlines with greater confidence requires accurately evaluating how the structural complexity of these ecosystems responds to environmental changes (Burns et al. 2015). Studies investigating wave dissipation across a reef have generally focused on collected field measurements of waves using relatively healthy reefs with high coral cover and biodiversity, and less steep reef faces (i.e., $>$ 1:10 steepness; e.g., Monismith et al. 2015; Quataert et al. 2015). As climate continues to warm, there will be a continuing shift in benthic composition toward reefs with lower coral cover and/or dominated by fewer, stress-tolerant coral species (Graham et al. 2015; Stuart-Smith et al. 2018), with potential consequences for reef structural complexity and wave attenuation.

The equatorial Gilbert Islands of the Republic of Kiribati, a series of populated low-lying atolls and reef islands exposed to frequent El Niño/Southern Oscillation (ENSO)-driven heat stress, are a unique and critical location to evaluate the effect of climate-driven shifts in benthic cover on reef ability to protect shorelines. In addition to frequent heat stress, the reefs of South Tarawa, the capital of Kiribati and home to over 50% of the country's population (63,439 inhabitants), have experienced high nutrient, sedimentation, and fishing pressure as well as mining of rock from reef flats for construction of homes and sea walls (Donner and Carilli 2019). However, benthic surveys find that resistance to heat stress is highest in South Tarawa reefs, rather than the less disturbed reefs of lightly populated North Tarawa and other neighboring atolls (Donner et al. 2010; Donner and Carilli 2019). The bleaching resistance at heavily disturbed sites is due to survival of a single opportunistic encrusting coral species, *Porites rus*, which has thrived despite exposure to sewage pollution and sediment loading (Cannon et al. 2021). The resilience of sites dominated by a single species with low morphological complexity suggests a possible trade-off between reef resilience to climate change and fore reef structural complexity. A possible decline in structural complexity is a key concern for atoll nations coping with the compounding effects of ocean warming, ocean acidification, sea-level rise, and local population pressure.

In this study, we investigate possible trade-offs between reef resilience and structural complexity, and the implications for reef ability to attenuate wave energy and protect shorelines, using in situ observations from Kiribati's Tarawa and Abaiang Atolls. The outer reefs of the two close neighboring atolls are an ideal location for this research, because their coral assemblages have responded differently to similar ENSO-driven heat stress over the past two decades. We first compute fore reef benthic cover and structural complexity for 16 sites across the two atolls using three-dimensional (3D) reconstructions of the fore reefs across all sites. We then evaluate relationships between fore reef benthic composition and structural complexity metrics and test for differences in structural complexity between atolls. In addition, to explore other potential influences on wave attenuation, we use a simple wave energy model (Sheppard et al. 2005) to estimate the effect of the fore reef slope and reef flat characteristics on wave attenuation. This analysis allows us to test the specific hypothesis that structural complexity is lower among the bleaching-resistant *Porites rus*-dominated reefs in South Tarawa, and to broadly assess the relevance for wave attenuation in light of human disturbances like reef flat mining.

Materials and methods

Study site

In April and May 2018, 3D reef structure was surveyed at 16 fore reef sites around the Republic of Kiribati's Tarawa (1°30' N, 173° E) (n = 10) and Abaiang (1°50' N, 173° E) (n = 6) Atolls in the central equatorial Pacific (Fig. 1; Table S1). The selected atolls are narrow and roughly two-thirds of the land is less than 2 m above mean sea-level (Woodroffe 2008; Aung et al. 2009). The field sites were chosen based on previous surveys, diversity of human disturbance and reef environments, and accessibility (Donner et al. 2010; Donner and Carilli 2019). Reef access is limited on the eastern rims of the atolls, which are exposed to open ocean swells; the North Tarawa site T05 and South Tarawa site T16, accessible during calm conditions, were included in this study in order to incorporate a wave-exposed site and a reef flat exposed to limited mining (T05). A local human disturbance metric was calculated for each site as the natural logarithm of the population of the nearest village divided by the distance to the center of the nearest village (Ministry of Finance and Economic Development 2016; Donner and Carilli 2019).

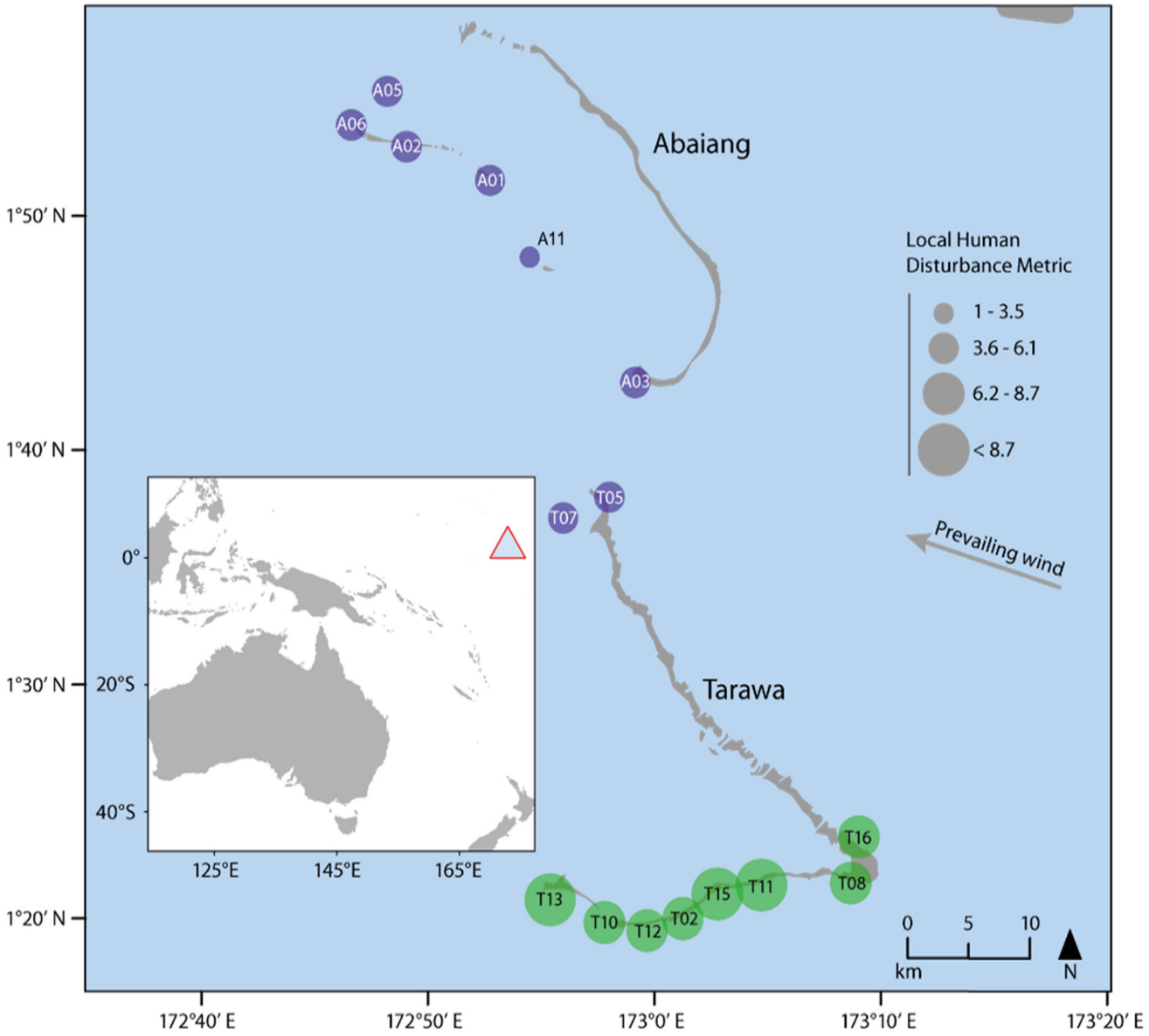

Fig. 1 Map of fore reef study sites around Tarawa and Abaiang, Republic of Kiribati. Sites in South Tarawa are shown in green and sites in North Tarawa and Abaiang are shown in purple. The sites are divided into four levels of local human disturbance metric. Inset shows the location of the Republic of Kiribati's Tarawa and Abaiang Atolls in the central equatorial Pacific Ocean

Benthic composition

Following a protocol used at these field sites since 2010, benthic composition and coral size structure were quantified using a single 50-m transect tape haphazardly laid along the fore reef at 10 m depth, with one transect per site (Donner and Carilli 2019). At 50-cm intervals along the transect, 0.33 m^2-sized quadrat photographs were taken and processed using Coral Point Count with Excel Extensions (CPCe) Research Software (version 4.1; Kohler and Gill 2006), following methods used in Cannon et al. (2019). Benthic cover was manually identified to the genus level for coral (with the exception of *Porites rus*) and macroalgae, and to functional groups for sponges, soft coral, algal turf, crustose coralline algae, and cyanobacteria. The sampling protocol was designed to capture the variance in the cover of common coral taxa at the field sites (Donner and Carilli 2019).

Structural complexity

At each site, high resolution images of the benthic substrate were collected over a 10 m × 10 m plot, situated such that the deep, seaward side lay in the middle of the 50-m transect. This design allowed the plot to be representative of the benthic cover of the site, following the established sampling protocol, as well as the slope of the site toward the reef crest while still maintaining a safe distance from the breaking waves. Diving weights were used as ground control points (GCPs) and were placed at the corners of the plot at known depths to enable accurate orthorectification of the resulting 3D reconstructions. A transect tape along the margin of the plot was also used to validate the spatial accuracy of the 3D models. Images of the reef substrate were collected with 70 to 80% overlap from both planar and oblique angles while swimming in a lawnmower pattern (Fig. S1) approximately 2 m above the substrate. Images were taken with a Canon PowerShot G7 X Mark II digital SLR camera with a 24-mm lens in a Fantasea FG7X II housing.

Images were processed using Agisoft Metashape to construct two-dimensional orthophotomosaics and 3D reconstructions of the reef plots. The SfM workflow generates a dense 3D point cloud that represents the structure of the substrate using x, y, and z data points, and a digital elevation model (DEM) that is a raster representing the 3D elevation of the substrate as a grid of cells. The ground sample distance (resolution/pixel) for all 3D reconstructions was less than 0.01 m/pix, and all the DEMs were rendered with a cell size of 1.0 cm, which is within the range of the ground sampling distance. The mosaics and DEMs are projected using the same local coordinate system, so they can be layered to perform identification and measurements of individual coral colonies. The model construction process follows details given by Burns et al. (2015).

Three geospatial metrics were quantified as proxies for structural complexity—surface rugosity, standard deviation of elevation, and terrain ruggedness—using the 3D analyst and spatial analyst tools in ArcMap (version 10.6.1). The raster cells of the DEM were set to 1 cm to capture the intricate structural differences among the various morphologies of the surveyed coral colonies. Surface rugosity (or tortuosity) was quantified as per Magel et al. (2019) and Carlot et al. (2020) for each reef plot and for all digitized polygons representing the benthic habitat. The standard deviation of elevation (SDE; or root mean square height) describes the variability of elevation values, here defined as within a 3 × 3 cell moving window (Leon et al. 2015). Higher values indicate areas of more pronounced vertical variation and thus more complex terrain. Terrain ruggedness was quantified using the 'benthic terrain modeler' tool in ArcMap as per Magel et al. (2019). This method encapsulates the variability in slope and aspect into a single value with values ranging from zero with no terrain variation to one with complete terrain variation (Sappington et al. 2007).

Benthic features were manually annotated on the orthophotomosaics following the procedure described by Burns et al. (2015). Unique polygon shapefiles were created for all individual living and recently dead major reef-building adult corals (≥ 5 cm diameter) and all sand patches in a smaller 8 m × 8 m plot within the larger 10 m × 10 m surveyed reef plot. A smaller plot was selected within each 3D model in order to account for variation in the size and shape of each surveyed reef plot. The reef building coral colonies (8,929 total adult coral colonies) were annotated following the categories *Acropora*, *Faviidae*, *Heliopora*, *Pocillopora*, *Porites rus*, massive *Porites*, other branching coral, and other massive coral; the classification is based on the most common coral taxa in the Gilbert Islands (Donner and Carilli 2019). We retain *Faviidae* as a category despite recent revisions to the taxonomy for consistency with previous data, and due to the commonality in morphology of the species present. For each 8 m × 8 m plot, the coverage of each of the taxa was calculated by determining the total area occupied by each taxa and dividing by the total area of the reef plot. The surface rugosity was also calculated for each adult coral.

To examine the relationship between the structural complexity of different coral morphologies, each major reef-building coral was assigned to one of three growth forms (Magel et al. 2019): branching (*Acropora*, *Heliopora*, *Pocillopora*, other branching coral), massive (*Faviidae*, massive *Porites*, other massive coral), or *Porites rus*. *Porites rus* was assigned its own morphology category

because it is dominant in South Tarawa reefs (Donner and Carilli 2019) and has a locally distinctive morphology (encrusting with plating and branching features). The coverage and surface rugosity of each of the three morphological categories was calculated using the methods outlined above for coral taxa, and statistically analyzed using ANOVA and Kruskal–Wallis tests and subsequent Tukey's Honestly Significant Difference post hoc test.

Coastal measurements

To examine the influence of other physical factors on wave energy reaching the shoreline, the reef flat width (W), surface roughness, and reef flat depth at high tide were measured at all Tarawa sites except T07, which is distant from land. Surveys were not carried out at the Abaiang sites or T07 since they were not adjacent to land or accessible (i.e., no roads nearby or private property). The reef flat width was measured using Google Earth and was calculated as the distance between the reef crest and the beach. To estimate surface roughness, in situ photographs were taken from the beach to the reef crest during low tide and then converted into friction factor (f_w) values (ranging from 0.08 for sand to 0.2 for rough uneroded coral) based on criteria outlined by Sheppard et al. (2005). The reef flat depth at high tide was estimated using standard trigonometric calculations based on visual observations of the high tide water line evidenced by the deposition of debris and algae.

The percent of offshore wave energy reaching the shoreline behind the reef was estimated at each Tarawa site (except T07) using a model developed by Sheppard et al. (2005). The model estimates wave energy at the shoreline based on inputs of reef profile factor (K_p), tangent angle of the reef face or rim (tan α_{reef}), offshore wave height (H_o), reef flat water depth (h_r), depth of reef edge (h_e), initial estimation of wave setup (n_r), atmospheric surge (n_w), beach slope gradient angle (tan α_{beach}), reef flat width (W), increment in wave height decay (d_x), and f_w on the reef flat. This one-dimensional spreadsheet based model was chosen, even though it does not incorporate the effects of fore reef surface roughness, because of the results of the structural complexity analysis (see "Results"), and because the input data necessary to execute a more advanced multi-dimensional hydrodynamic model were not physically possible to collect at these exposed and remote field sites.

For all sites, H_o was set at 1.5 m, based on the mean value from NOAA's Wavewatch III model during the 2009–2010 boreal winter when Tarawa experienced ENSO-driven high waves and shoreline damage. The h_r was set at 1.41 m based on the 2018 mean tidal range in Betio, Kiribati, available from the Australian Bureau of Meteorology. All reef flats were standardized with a tan α_{beach} of 0.125, tan α_{reef} of 0.036, and d_x of 5, based on inputs for other reef-lined shorelines (Sheppard et al. 2005). The values for W and f_w were modified according to the coastal measurements above. Estimates for K_p were based on the fore reef slope of each site computed from the photomosaic and the corresponding K_p value outlined in Table 2 of Sheppard et al. (2005).

Statistical analyses

Statistical analyses were conducted using R version 3.5.1 (R Core Team 2019). Information-theoretic model selection procedures were used to examine the influence of local stressors, as represented by the human disturbance metric and the variability of maximum SST (Donner 2011), on coral reef surface rugosity, standard deviation of elevation, and terrain ruggedness. For each structural complexity metric, linear mixed-effects (LME) models were fit with local human disturbance and the density of each of the coral morphologies used as fixed effects and atoll as a random effect (to account for non-independence among sites at the same atoll). Since the coral cover for each of the growth forms calculated using the photomosaics and quadrat photos was highly correlated ($p < 0.001$), only the data quantified from the photomosaics were used for the models. Prior to statistical modelling, all fixed effects variables were standardized to a mean of zero and a standard deviation of one using the function 'rescale' (in package *arm;* Gelman and Yu-Sung 2018) to allow for comparison of the effect sizes of different variables (Gelman 2008). The coefficient of variability of maximum annual SST (CV_{SST}) for each of the field sites was computed using 1985 to 2017 daily SST data from NOAA Coral Reef Watch's CoralTemp V1.0 dataset. We explored the possibility of including CV_{SST} as a fixed effect; however, this was ultimately deemed to be unnecessary because of the similarity of CV_{SST} across the sampled sites.

For each structural complexity metric, 15 models were evaluated by fitting every combination of variables (Table S2). The small-sample corrected Akaike information criterion (AICc) was used to compare models and estimate the magnitude of differences between models with respect to expected predictive power. The AIC_c values were also used to produce a set of all reasonably well-fitting models that are within 10 ΔAIC_c of the best model (Bolker et al. 2008). Within the set of reasonably well fit models, model-averaged parameter estimates and 95% confidence intervals for each predictor variable were calculated in order to account for model uncertainty. The relative variable importance (RVI) of individual parameters was also determined using the function 'importance' by calculating the sum of the Akaike weights across all models containing a given parameter with the most

important parameter having a maximum possible value of one. Models were fit using the R package *nlme* (Pinheiro et al. 2019), and information-theoretic model selection was performed using the package *MuMIn* (Barton 2019). As in previous studies, for many analyses North Tarawa sites are grouped with Abaiang sites due to their close proximity and similar level of human disturbance (Donner and Carilli 2019).

In addition to our linear mixed-effects models, a variance partitioning analysis was used to determine the variance explained by local human disturbance and the densities of branching, massive, and *Porites rus* corals for each complexity metric, and to test for robustness of the results given collinearity between variables. Permutation tests (n = 1,000) were used to determine whether the predictor variables explained significant amounts of variation in the structural complexity metrics. Redundancy analysis (RDA) and variance partitioning were implemented using the *rda* and *varpart* functions in the *vegan* package version 2.5–7 (Oksanen et al. 2020).

Results

Coral reef community composition across sites

The surveys find notable differences in the typical fore reef coral community compositions between sites in South Tarawa and sites in North Tarawa and Abaiang (Fig. 2), as noted in earlier work (Donner and Carilli 2019). Reefs in South Tarawa, on average, had a higher live coral cover (34%) than sites in North Tarawa and Abaiang (17%). North Tarawa and Abaiang had significantly more *Halimeda* spp. (Kruskal–Wallis $H = 12.88$, $df = 1$, $p < 0.001$), while sites in South Tarawa had significantly more cyanobacteria ($H = 8.90$, $df = 1$, $p < 0.01$; Fig. 2a). There were also site-specific differences in the coral community composition with sites in South Tarawa, on average, having lower species evenness relative to sites in North Tarawa and Abaiang (Fig. 2b). *Porites rus* dominated reefs in South Tarawa ($H = 12.18$, $df = 1$, $p < 0.001$) with a median of 91% of relative coral cover, with the exception of site T16, the South Tarawa site most exposed to open ocean swells. We found no sites in South Tarawa with branching *Acropora* spp. and few with massive *Porites* and *Favidae*. In contrast, sites in North Tarawa and Abaiang were dominated by *Heliopora*, *Favidae*, massive *Porites*, and *Acropora*.

Structural complexity across sites

The fore reef surface rugosity and SDE were not significantly different between the atolls (Fig. 3). The terrain

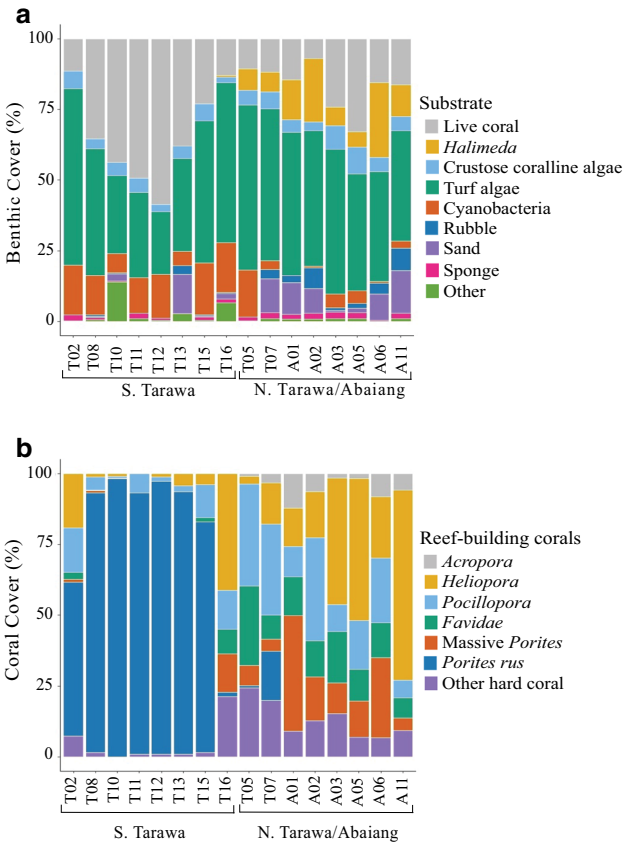

Fig. 2 Benthic cover of **a** key benthic categories and **b** major reef-building corals at each study site

ruggedness was significantly higher ($F = 5.67$, $df = 1$, $p = 0.03$) at the South Tarawa sites than at the North Tarawa and Abaiang sites, although the difference was small (0.11 ± 0.02 vs. 0.09 ± 0.01; mean $\pm$ SD). On average, sites with a lower human disturbance metric had a lower average surface rugosity and terrain ruggedness. The average local human disturbance value of the South Tarawa sites (8.02 ± 0.79; mean $\pm$ SD) was significantly higher ($F = 32.72$, $df = 1$, $p < 0.001$) than that of the North Tarawa and Abaiang sites (4.97 ± 0.87; mean $\pm$ SD). As such, sites which experience greater local disturbance had a higher overall reef structural complexity than sites that are further from a village or area with dense population.

Coral taxa contribute differentially to structural complexity

We examined the surface rugosity of individual features to understand their relative contribution to overall structural complexity at each site. Surface rugosity of individual corals is influenced to a considerable extent by coral morphology (One-way ANOVA; $F = 16.95$, $df = 2$, $p < 0.001$). Branching corals had a higher mean surface

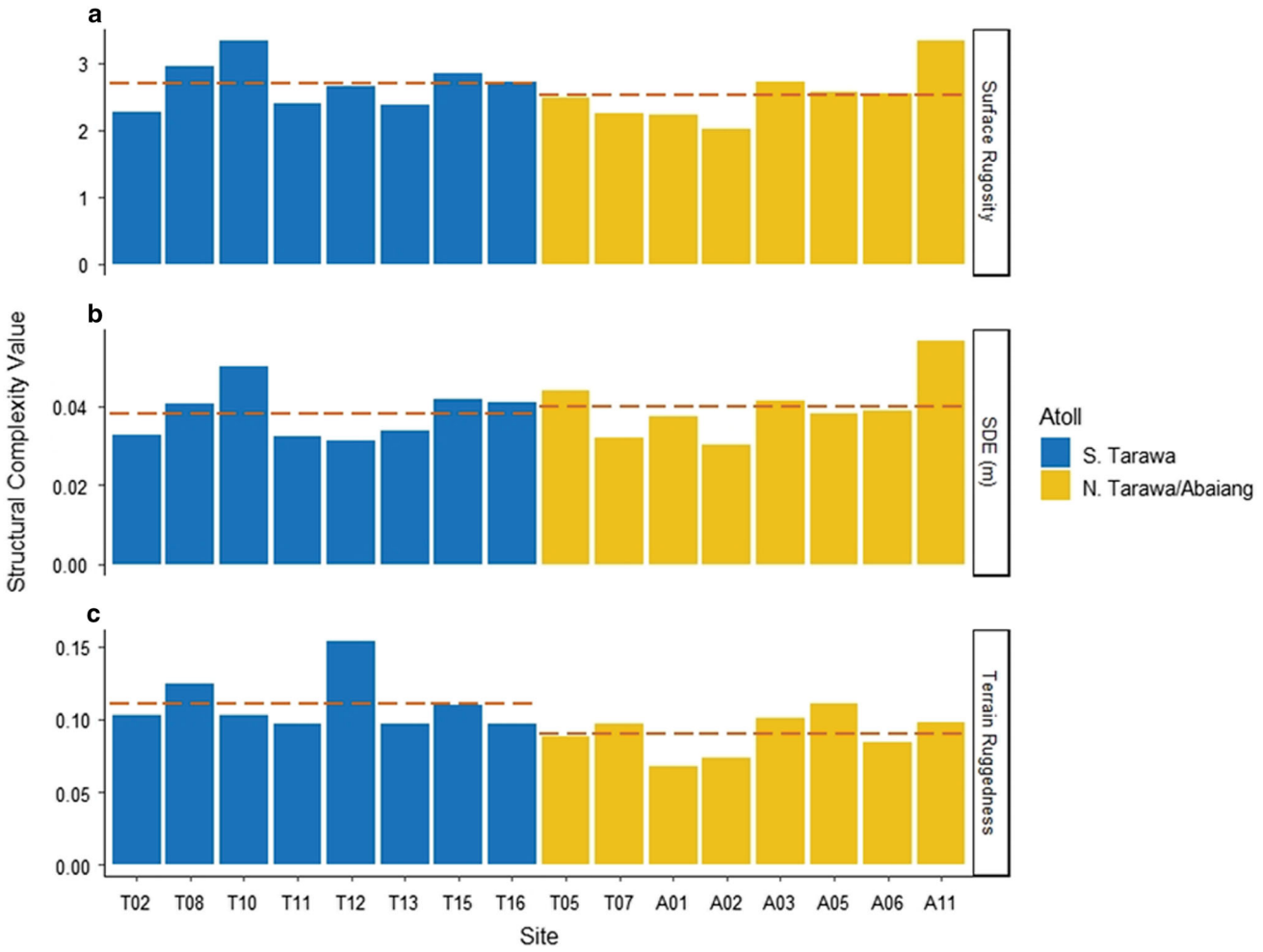

Fig. 3 Structural complexity characterization of fore reef plots across 16 reef sites in Tarawa and Abaiang Atolls, Kiribati. The three complexity metrics are **a** surface rugosity, **b** standard deviation of elevation (SDE), and **c** terrain ruggedness. Orange dashed line represents the mean for each atoll

rugosity relative to the massive corals (Tukey's HSD; $p < 0.001$) and *Porites rus* ($p = 0.01$,; Fig. 4), but there was no significant difference between massive corals and *Porites rus*. Although *Porites rus* does not have as high a surface rugosity compared to branching corals, *Porites rus* contributes greatly to the overall surface rugosity of site T10 because it dominates the coral cover of the fore reef at that site (Fig. 2b). In contrast, although site A02 had a higher diversity of coral taxa (Fig. 2b), the coverage of branching corals (i.e., *Heliopora*, *Pocillopora*) was lower compared to sites A05 and A11, with the reduced coverage resulting in a lower estimate of overall reef surface rugosity. It is important to note that the mean surface rugosity of each coral taxon is variable between sites, with certain taxa having high surface rugosity values (i.e., surface rugosity > 4) at some but not all sites (Fig. S2).

Drivers of structural complexity

The linear mixed-effects models (Fig. 5) indicate that reef structural complexity in Tarawa and Abaiang is predominantly determined by a combination of branching and *Porites rus* coral cover. The strongest predictors varied between surface rugosity, SDE, and terrain ruggedness, with no single predictor variable consistently explaining the reef structural complexity across all three metrics. However, branching and *Porites rus* coral cover were the strongest predictors of surface rugosity (Fig. 5a) with a relative variable importance (RVI) of 0.51 and 0.4, respectively (Table S3). None of the predictor variables had a strong effect on SDE (Fig. 5b), with the most important parameter, branching coral, only generating an RVI of 0.29 (Table S4). The coverage of *Porites rus* and branching corals were the most important predictors of reef terrain ruggedness with an RVI of 0.91 and 0.55, respectively (Table S5). The abundance of *Porites rus* was a

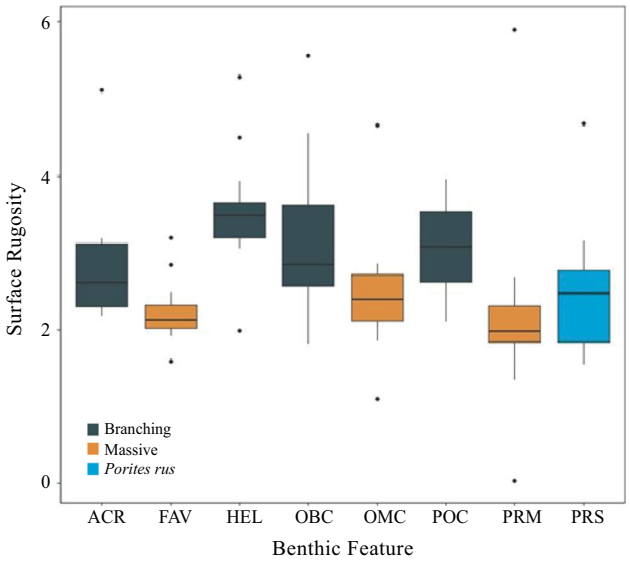

Fig. 4 Comparisons between the mean surface rugosity of key reef building coral taxa across fore reef sites in Tarawa and Abaiang Atolls, Kiribati. ACR = *Acropora*, FAV = *Favidae*, HEL = *Heliopora*, OBC = Other Branching Coral, OMC = Other Massive Coral, POC = *Pocillopora*, PRM = *Porites* Massive, PRS = *Porites rus*

significant positive predictor of terrain ruggedness and not surprisingly sites with greater coverage of *Porites rus* (i.e., sites around South Tarawa) were associated with a higher terrain ruggedness (Fig. 5c). The abundance of branching corals had a weak positive influence on all three structural complexity metrics as shown by the 95% confidence intervals overlapping zero. Local human disturbance and massive coral cover had very weak influences on all three structural complexity metrics, with rugosity and SDE slightly lower on reefs with a higher local disturbance value. We repeated the LME analysis using additional variables, CV_{SST} and average water depth of the fore reef plot, and found both variables did not contribute strongly to any of the three complexity metrics.

Variance partitioning analysis confirmed that the conditional effect of *Porites rus* and branching coral cover explained the most variance in surface rugosity, 20.7% and 14.2%, respectively (adjusted R^2; Fig. 6a and Table S6). In addition, 28.7% of the explained variation in rugosity was an interactive effect between the cover of *Porites rus* and branching corals ($p = 0.045$; Table S7). The conditional effect of *Porites rus* and branching coral cover explained 25.5% and 15.8% of the variation in terrain ruggedness, while the shared variance of local human disturbance and *Porites rus* and massive coral cover was 19.7% (Fig. 6c). For both surface rugosity and terrain ruggedness, the shared variance of *Porites rus* and massive coral cover explained 13.4% and 13.8% of the variance (Fig. 6a,c). Lastly, 38.4% of the explained variation in terrain ruggedness was attributable to *Porites rus* ($p = 0.08$) and the models for terrain ruggedness that had the variable *Porites rus* were significant by permutation analysis (Table S7). The shared variance of local human disturbance and massive and branching coral cover explained the most variance in SDE at 10.4% (Fig. 6b); however, permutation testing found that the models were not significant (Table S7).

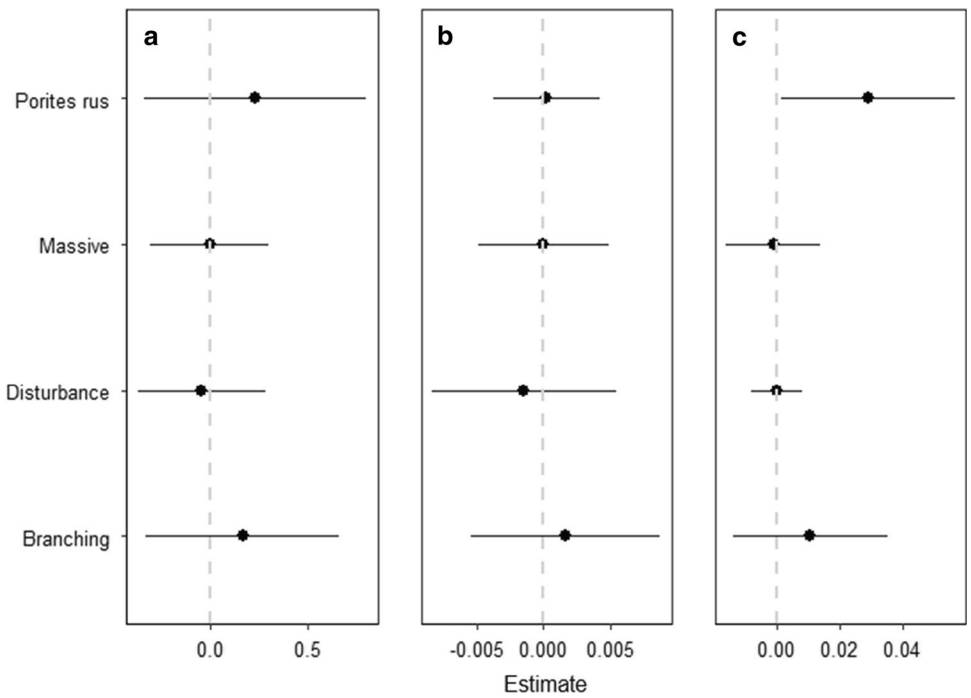

Fig. 5 Multi-model-averaged parameter estimates and 95% confidence intervals for predictors of **a** surface rugosity, **b** standard deviation of elevation (SDE), and **c** terrain ruggedness

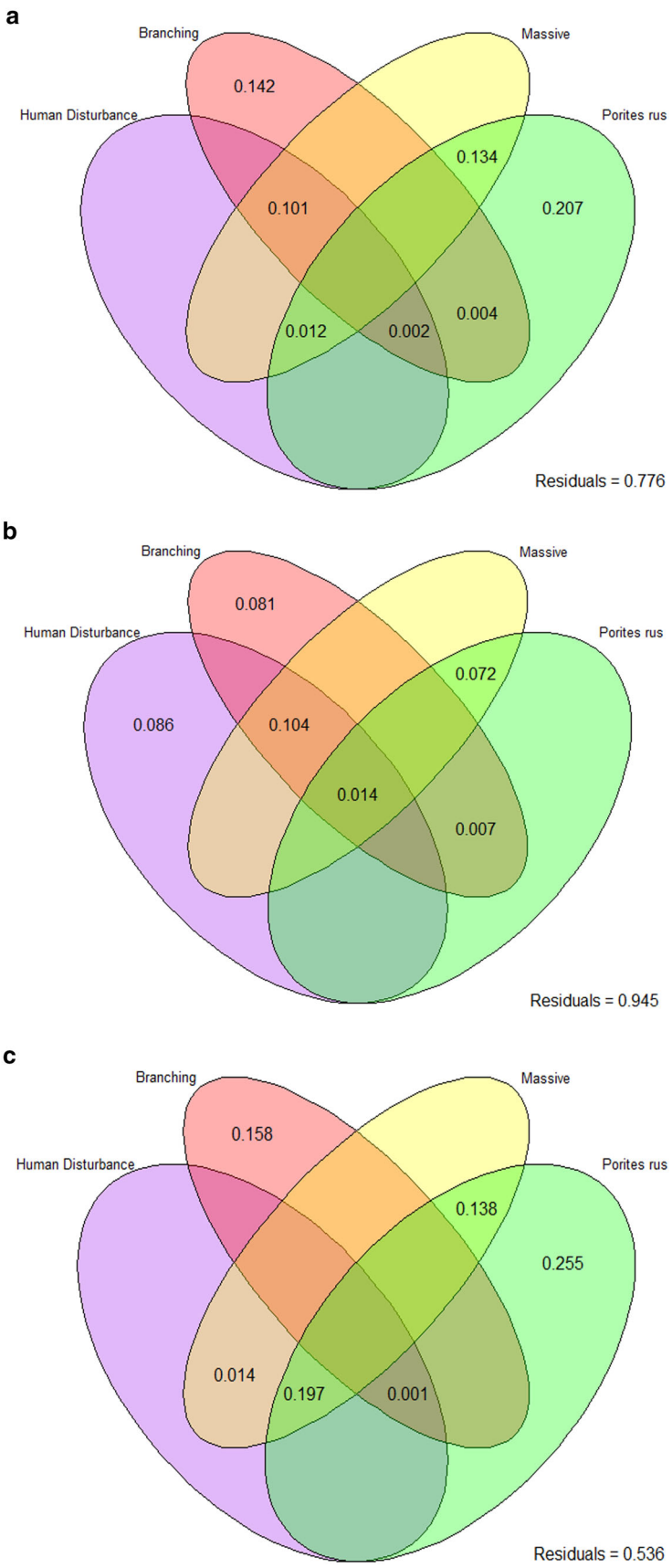

Fig. 6 Variance partitioning for **a** surface rugosity, **b** standard deviation of elevation (SDE), and **c** terrain ruggedness. The total adjusted R^2 and the amount of variation attributed to human disturbance, branching coral cover, massive coral cover, and *Porites rus* coral cover and the interaction between them for the complexity metrics. Variance components < 0.001 not shown

Other influences on wave attenuation

Beach surveys found similar reef flat width and water depth at the South Tarawa sites and the North Tarawa site, but a large difference in the reef flat surface roughness (Table 1). The reef flats around South Tarawa (Fig. 7a) are predominantly smooth rock with 75% to 100% coverage by seagrass or algal turf, or sand and with less than 30% dead, but not eroded coral or boulders. By contrast, the reef flat in North Tarawa (T05) was predominantly (80%) dead intact coral or boulders greater than 30 cm (Fig. 7b). This site was broadly representative of reef flats around the north end of Tarawa where there has been limited mining of reef rock.

Based on the reef flat roughness characterizations by Sheppard et al. (2005), the reef flats in South Tarawa had an average f_w of 0.1 compared to the reef flat in North Tarawa with an f_w of 0.2. Based on the wave energy model by Sheppard et al. (2005), sites in South Tarawa had, on average, 13% of the offshore wave energy reach the shoreline behind each reef while the North Tarawa site had only 8% of the offshore wave energy reach shore. In order to evaluate the effect of reef flat mining, we repeated the model runs for South Tarawa using the bottom roughness of the North Tarawa site. When sites in South Tarawa were assigned an f_w value similar to the North Tarawa site, wave energy dissipation increased from 87 to 92% (Table S8). Conversely, if the f_w value is increased to that of a 75–100% sand bottom, the South Tarawa reefs dissipate 4% less wave energy while the North Tarawa reefs would dissipate 9% less wave energy (Table S8). As such, if the reef flats around North Tarawa were to be mined leaving only a sandy substrate, 17% of the offshore wave energy would be expected to reach the shoreline compared to the 8% at present. Overall, reef flats with a higher roughness will attenuate more offshore wave energy from reaching the shore.

Discussion

Reefs with higher diversity of living corals have long been generally assumed to also be more complex (Chabanet et al. 1997; Bruno and Bertness 2001). A greater diversity of physical habitats, however, does not necessarily translate into a greater overall structural complexity; a thicket of *Acropora formosa* can have higher structural complexity than a reef of multiple species and growth forms. This study finds greater or equivalent structural complexity at more homogenous, bleaching-resistant reef sites in South Tarawa compared to the more diverse sites in Abaiang and North Tarawa. The South Tarawa reefs, unlike the Abaiang and North Tarawa reefs, have maintained relatively high coral cover despite multiple heat stress events over the past twenty years due to the persistence and expansion of a single bleaching-resistant coral species (Donner and Carilli 2019; Cannon et al. 2021). At these sites, reef complexity increases with coral cover although the relationship depends on the morphological and functional traits of the dominant coral species. As such, the generally accepted, positive association between diversity and structural complexity may not be universal but more context specific. The type and dominance of key reef-building corals can be just as important as their overall abundance in maintaining reef structural complexity, as proposed by Alvarez-Filip et al. (2011). Below we discuss the findings in more detail and the implications for measuring structural complexity and for shoreline protection provided by coral reefs.

Structural complexity differs by metric, coral morphology, and across atoll

Consistent methods for measuring structural complexity are important given the role of structural complexity in promoting recovery from disturbances (Graham et al. 2015) and in dissipating wave energy (Monismith et al.

Table 1 Comparison between reef characteristics across atolls

Reef characteristic	South Tarawa	North Tarawa
Fore reef slope	Steeper (avg. = 1:7)	Gentle (avg. = 1:13)
Fore reef bottom roughness	Higher terrain ruggedness	Lower terrain ruggedness
(i.e., structural complexity)	No significant differences in surface rugosity and SDE	
Fore reef coral biodiversity	Low species evenness	Higher species evenness
Fore reef live coral cover	Higher (avg. = 34%)	Lower (avg. = 17%)
Reef flat width	Wide (avg. = 317.5 m)	Wide (205 m)*
Reef flat water depth	Shallow (avg. = 1.75 m)	Shallow (1.8 m)*
Reef flat bottom roughness (f_w)	Smooth (avg. = 0.1)	Rough (0.2)*

*Data based on one North Tarawa reef flat (site T05)

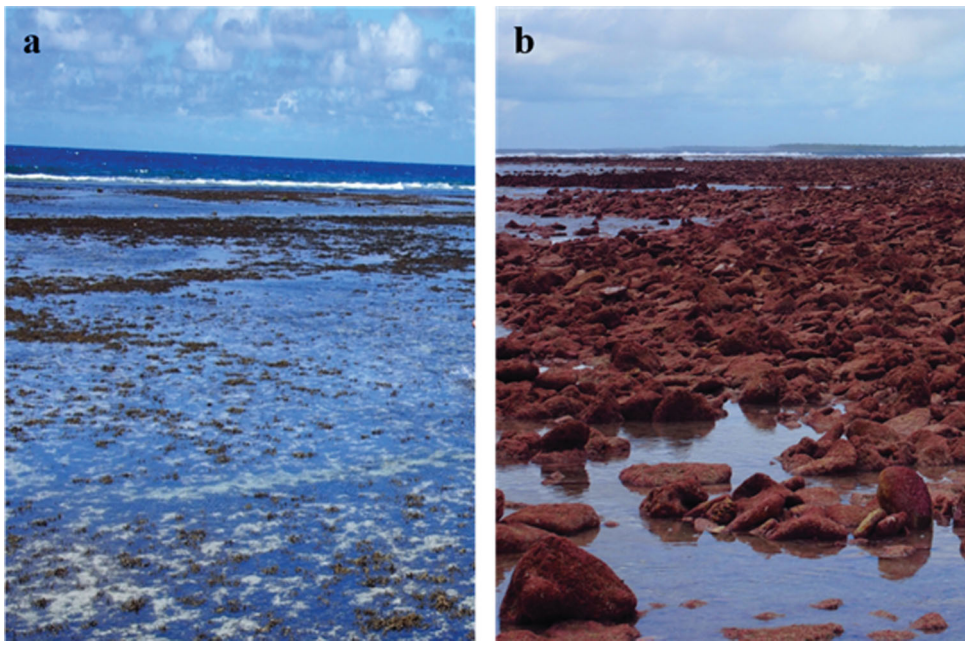

Fig. 7 Typical reef flat topography visible at low tide in **a** South Tarawa and **b** North Tarawa

2015). Through the SfM photogrammetry analysis, we found that the relative difference in structural complexity between the atolls was dependent upon the metric used to measure complexity. Specifically, the surface rugosity and SDE were not different between atolls, while the average terrain ruggedness was significantly greater at the South Tarawa sites, in particular sites T12 and T08. Furthermore, through the effect size analysis, we determined that the abundance of *Porites rus* and branching corals was positively related for all three complexity metrics, with the strongest positive association between *Porites rus* and terrain ruggedness. Terrain ruggedness is likely better able to capture the fine-scale morphologies of branching and plating forms of *Porites rus*, and therefore the metric was highest at sites around South Tarawa where *Porites rus* is dominant.

A number of studies have also reported significant relationships between overall coral cover and structural complexity (Alvarez-Filip et al. 2011; Darling et al. 2017; Magel et al. 2019; Price et al. 2019; Carlot et al. 2020). In contrast to previous studies (Alvarez-Filip et al. 2011; Magel et al. 2019), we did not find a significant relationship between massive coral cover and any of the reef complexity metrics. The lack of a significant relationship may be related to the specific history and the massive coral assemblage at these sites. The mean coral size was small in the 2018 surveys, particularly at Abaiang Atoll, because massive species were affected by a 2013–2014 outbreak of the corallivorous sea starfish *Acanthaster cf solaris*, or Crown-of-Thorns, in addition to heat stress events (Cannon et al. 2021). The massive and submassive coral assemblages around Tarawa and Abaiang Atolls are also dominated by *Porites lutea* and *Porites lobata*, which have more rounded surfaces with less fine-scale roughness relative to some of the massive coral species noted in other studies (*Montastraea* around Cozumel, Mexico, Alvarez-Filip et al. 2011; columnar or ridge-like structures in Kiritimati, Magel et al. 2019). Given the rounded dome structure of many massive coral genera, the contribution of massive corals to measures of reef complexity may also depend strongly on the scale at which complexity is quantified. The large-scale complexity of massive coral assemblages may not contribute as strongly as the fine-scale roughness of branching coral assemblages given the calibration scale that we used in this study.

Through the mixed-effects models and variance partitioning, we also found that while surface rugosity and SDE were slightly lower on reefs with a higher local disturbance value, the statistical relationship was weak. In contrast, Magel et al. (2019) found that structural complexity of fore reefs that have undergone heat stress declined with increasing levels of human disturbance. As noted above, nutrient loading and sedimentation in South Tarawa likely contributed to the spread of *Porites rus* (Lovell et al. 2001; Donner and Carilli 2019; Cannon et al. 2021), a resilient opportunistic and generalist coral species (Darling et al. 2012). *Porites rus* is able to adjust to changes in environmental conditions on short time scales (weeks) through expression of attributes that maximize colony energy acquisition (Padilla-Gamiño et al. 2012). Although the *Porites rus*-dominated reefs are as or more structurally complex than the North Tarawa and Abaiang reefs, it remains to be seen whether these corals will be able to vertically accrete fast enough to keep pace with rising sea

levels (Perry and Morgan 2017; Perry et al. 2018), particularly given changing ocean carbonate chemistry (Kline et al. 2019). Several recent studies have computed that a shift to opportunistic, bleaching-resistant coral species resulted in losses in coral-community calcification and thus declined in reef structural complexity (Alvarez-Filip et al. 2013; Lange and Perry 2019; Courtney et al. 2020).

Coastal protection provided by reefs

Rising sea levels and wave-induced inundation threaten the freshwater resources, agriculture, and the habitability of low-lying atoll nations like Kiribati (Woodroffe 2008; Storlazzi et al. 2018). Coral reefs can help mitigate impacts of severe storm surges and limit coastal erosion in atolls and other reef islands (Ferrario et al. 2014). The interaction between sea level, waves, and reef properties such as topography, roughness, and size governs nearshore hydrodynamics on atolls and together influences the extent to which islands are impacted by an encroaching sea.

Ideally, a two-dimensional hydrodynamic model like XBeach would be used to evaluate the influence of the measured fore reef structural complexity on wave attenuation relative to that of other important reef properties (e.g., reef flat depth and roughness). Given the inability to collect the required input data for a hydrodynamic model at these field sites (Donner and Carilli 2019), and the unexpected similarity in structural complexity metrics between the South Tarawa sites and all other sites, we instead employed the simple Sheppard et al. (2005) model to broadly explore influence of factors other than fore reef roughness on wave attenuation. The model indicated that lower bottom roughness of the South Tarawa reef flats, relative to the North Tarawa site, allows more offshore wave energy to reach shore. The South Tarawa reef flats once resembled the rougher reef flat in North Tarawa (see Forbes and Hosoi 1995), but human activities including beach and reef flat mining for homes and seawalls have resulted in a loss of boulders (Biribo and Woodroffe 2013). We estimate the loss of boulders from reef flats in South Tarawa have contributed toward a 5% increase in wave energy. The increase in offshore wave energy reaching shorelines (i.e., wave runup) with low bottom friction on the reef flat follows from the results of past models and measurements (Quataert et al. 2015; Yao et al. 2019).

The smoother reef flats as well as the steeper fore reef slopes on South Tarawa reefs relative to most North Tarawa and Abaiang reefs likely lead to higher wave energy reaching the South Tarawa shorelines, despite the higher coral cover and higher associated wave energy attenuation in South Tarawa (Table 1). Using field data and a calibrated model, Quataert et al. (2015) found that steep fore reef slopes ($\sim$ 1:10 and steeper) increased wave runup and intensified coastal erosion and flooding. Although the slope measurements could be biased by placement of the 10 m $\times$ 10 m at a safe diving distance from the reef crest, the reported relative difference in slope between South Tarawa and most North Tarawa and Abaiang reefs agrees that of with past visual surveys (e.g., Lovell et al. 2001; Donner et al. 2010).

These findings illustrate that more research is needed to establish how wave attenuation by fore reefs is altered by bleaching-driven regime shifts to fewer and/or opportunistic coral species. This requires bridging the gap between the biological and ecological in situ measurements of structural complexity indices (rugosity, SDE, and terrain ruggedness) using 3D photogrammetry and the hydrodynamic models that use bottom friction (f_w and c_f). Despite parallel advances in developing 3D reef models based on SfM photogrammetry techniques and in nearshore wave and sediment dynamic models such as XBeach, there is still no satisfactory method of measuring reef roughness (i.e., structural complexity) that can be transformed into hydrodynamic parameters like f_w (Monismith 2007; Monismith et al. 2015). One solution is for researchers planning photo surveys for the purpose of developing 3D reef models to also install pressure sensors on cross-shore transects, in order to monitor site-specific changes in offshore wave energy along the entire reef as in Quatert et al. (2015). In addition, building off the flume laboratory experiments conducted by Yao et al. (2019), 3D models generated from the SfM photogrammetry could be used to 3D-print coral reefs scaled to a wave flume which would then be used to empirically test the effect of realistic fore reef morphology on wave processes over a reef. These future wave experiments may provide greater insights into the effects of more disturbed and less diverse reefs on wave attenuation.

In summary, at the current sea level, the low diversity of coral growth forms on the fore reef in Tarawa and Abaiang will likely not substantially affect the reef's capacity to attenuate wave energy as much as factors like coral cover, steepness of the fore reef, and composition of the reef flat. Although the coral cover and terrain ruggedness were higher at most of the South Tarawa sites relative to the North Tarawa and Abaiang sites, we expect the beneficial influences of these parameters on shoreline protection will not outweigh the adverse effects of the steep fore reef slopes and smooth reef flats around South Tarawa (Table 1). Our research provides an improved understanding of the reef structure around Tarawa and Abaiang that can be used to inform future studies in the Pacific, as well as ongoing reef monitoring and management in Kiribati.

Supplementary Information The online version contains supplementary material available at https://doi.org/10.1007/s00338-022-02238-7.

Acknowledgements The authors thank Max Peter, Erietera Aram, Toaea Beiateuea, Tooreka Teemari, and Karibanang Tamuera of the Kiribati Ministry of Fisheries and Marine Resource Development (MFMRD) for their assistance in the field and facilitation of the research. We also thank the Ministry of Environment, Lands, and Agricultural Development for providing approval for the field surveys. The authors would also like to thank Sara Cannon for her assistance in the field and CPCe photo analysis. This work was supported by a Natural Sciences and Engineering Research Council of Canada (NSERC) Discovery Grant (SDD), a NSERC Ship Time Extension (SDD), and a NSERC Canada Graduate Scholarship (HES).

Author contributions SDD conceived of the study, HES and SDD collected the data, and HES performed the analysis and wrote the text with the assistance of SDD.

Data availability The datasets generated during and/or analyzed during the current study are available in the Zenodo repository, https://doi.org/10.5281/zenodo.5093789.

References

Alvarez-Filip L, Dulvy NK, Côté IM, Watkinson AR, Gill JA (2011) Coral identity underpins architectural complexity on Caribbean reefs. Ecol Appl 21:2223–2231

Alvarez-Filip L, Carricart-Ganivet JP, Horta-Puga G, Iglesias-Prieto R (2013) Shifts in coral-assemblage composition do not ensure persistence of reef functionality. Sci Rep. https://doi.org/10.1038/srep03486

Aung T, Singh A, Prasad U (2009) A study of sea-level changes in the Kiribati area for the last 16 years. Weather 64:203–206

Barton K (2019) MuMIn: multi-model inference. R package version 1.43.6. https://CRAN.R-project.org/package=MuMIn

Biribo N, Woodroffe CD (2013) Historical area and shoreline change of reef islands around Tarawa Atoll, Kiribati. Sustain Sci 8:345–362

Bolker BM, Brooks ME, Clark CJ, Geange SW, Poulsen JR, Stevens MHH, White JS (2008) Generalized linear mixed models: a practical guide for ecology and evolution. Trends Ecol Evol 24:127–135

Bruno JF, Bertness MD (2001) Habitat modification and facilitation in benthic marine communities. In: Bertness MD, Gaines SD, Hay ME (eds) Marine Community Ecology. Sinauer, Sunderland, pp 201–218

Burns JHR, Delparte D, Gates RD, Takabayashi M (2015) Integrating structure-from-motion photogrammetry with geospatial software as a novel technique for quantifying 3D ecological characteristics of coral reefs. PeerJ. https://doi.org/10.7717/peerj.1077

Cannon SE, Donner SD, Fenner D, Beger M (2019) The relationship between macroalgae taxa and human disturbance on central Pacific coral reefs. Mar Pollut Bull 145:161–173

Cannon SE, Aram E, Beiateuea T, Kiareti A, Peter M, Donner SD (2021) Coral reefs in the Gilbert Islands of Kiribati: resistance, resilience and recovery after more than a decade of multiple stressors. PLoS ONE 16(8):e0255304. https://doi.org/10.1371/journal.pone.0255304

Carlot J, Rovère A, Casella E, Harris D, Grellet-Muñoz C, Chancerelle Y, Dormy E, Hedouin L, Parravicini V (2020) Community composition predicts photogrammetry-based structural complexity on coral reefs. Coral Reefs 39:967–975

Chabanet P, Ralambondrainy H, Amanieu M, Faure G, Galzin R (1997) Relationships between coral reef substrata and fish. Coral Reefs 16:93–102

Cornwall CE, Comeau S, Kornder NA, Perry CT, van Hooidonk R, DeCarlo TM, Pratchett MS, Anderson KD, Browne N, Carpenter R, Diaz-Pulido G, D'Olivo JP, Doo SS, Figueiredo J, Fortunato SAV, Kennedy E, Lantz CA, McCulloch MT, González-Rivero M, Schoepf V, Smithers SG, Lowe RJ (2021) Global declines in coral reef calcium carbonate production under ocean acidification and warming. Proc Nat Acad Sci USA 118(21):e2015265118. https://doi.org/10.1073/pnas.2015265118

Costa M, Macedo E, Siegle E (2019) Wave refraction and reef island stability under rising sea level. Glob Planet Chang 172:256–267

Couch CS, Burns JHR, Liu G, Steward K, Gutlay TN, Kenyon J, Eakin CM, Kosaki RK (2017) Mass coral bleaching due to unprecedented marine heatwave in Papahānaumokuākea Marine National Monument (Northwestern Hawaiian Islands). PLoS ONE. https://doi.org/10.1371/journal.pone.0185121

Courtney TA, Barnes BB, Chollett I, Elahi R, Gross K, Guest JR, Kuffner IB, Lenz EA, Nelson HR, Rogers CS, Toth LT, Andersson AJ (2020) Disturbances drive changes in coral community assemblages and coral calcification capacity. Ecosphere. https://doi.org/10.1002/ecs2.3066

Darling ES, Alvarez-Filip L, Oliver TA, McClanahan TR, Côté IM (2012) Evaluating life-history strategies of reef corals from species traits. Ecol Lett 15:1378–1386

Darling ES, Graham NAJ, Januchowski-Hartley FA, Nash KL, Pratchett MS, Wilson SK (2017) Relationships between structural complexity, coral traits, and reef fish assemblages. Coral Reefs 36:561–575

Donner SD (2011) An evaluation of the effect of recent temperature variability on the prediction of coral bleaching events. Ecol Appl 21:1718–1730

Donner SD, Carilli J (2019) Resilience of Central Pacific reefs subject to frequent heat stress and human disturbance. Sci Rep. https://doi.org/10.1038/s41598-019-40150-3

Donner SD, Kirata T, Vieux C (2010) Recovery from the 2004 coral bleaching event in the Gilbert Islands. Kiribati Atoll Res Bull. https://doi.org/10.5479/si.00775630.587

Ferrario F, Beck MW, Storlazzi CD, Micheli F, Shepard CC, Airoldi L (2014) The effectiveness of coral reefs for coastal hazard risk reduction and adaptation. Nat Commun. https://doi.org/10.1038/ncomms4794

Forbes DI, Hosoi Y (1995) Coastal erosion in South Tarawa, Kiribati. SOPAC Tech Rep 255:1–91

Gelman A (2008) Scaling regression inputs by dividing by two standard deviations. Stat Med 27:2865–2873

Gelman A, Yu-Sung S (2018) arm: data analysis using regression and multilevel/hierarchical models. R package version 1.10–1. https://CRAN.R-project.org/package=arm

Gourlay MR, Colleter G (2005) Wave-generated flow on coral reefs – an analysis for two-dimensional horizontal reef-tops with steep faces. Coast Eng 52:353–387

Graham NAJ, Nash KL (2013) The importance of structural complexity in coral reef ecosystems. Coral Reefs 32:315–325

Graham NAJ, Jennings S, MacNeil A, Wilson MD, SK, (2015) Predicting climate-driven regime shifts versus rebound potential in coral reefs. Nature 518:94–97

Harris DL, Rovere A, Casella E, Power H, Canavesio R, Collin A, Pomeroy A, Webster JM, Parravicini V (2018) Coral reef structural complexity provides important coastal protection from waves under rising sea levels. Sci Adv. https://doi.org/10.1126/sciadv.aao4350

Kench PS, Brander RW (2006) Wave processes on coral reef flats: implications for reef geomorphology using Australian Case Studies. J Coast Res 221:209–223

Kline DI, Teneva L, Okamoto DK, Schneider K, Caldeira K, Miard T, Chai A, Marker M, Mitchell BG, Dove S, Hoegh-Guldberg O (2019) Living coral tissue slows skeletal dissolution related to ocean acidification. Nat Ecol Evol 10:1438–1444

Kohler KE, Gill SM (2006) Coral point count with excel extensions (CPCe): a visual basic program for the determination of coral and substrate coverage using random point count methodology. Comput Geosci 32:1259–1269

Lange ID, Perry CT (2019) Bleaching impacts on carbonate production in the Chagos Archipelago: influence of functional coral groups on carbonate budget trajectories. Coral Reefs 38:619–624

Leggat WP, Camp EF, Suggett DJ, Heron SF, Fordyce AJ, Gardner S, Deakin L, Turner M, Beeching LJ, Kuzhiumparambil U, Eakin CM, Ainsworth TD (2019) Rapid coral decay is associated with marine heatwave mortality events on reefs. Curr Biol 19:2723–2730

Leon JX, Roelfsema CM, Saunders MI, Phinn SR (2015) Measuring coral reef terrain roughness using 'Structure-from-Motion' close-range photogrammetry. Geomorphology 242:21–28

Lovell ER, Kirata T, Tekinaiti T (2001) Status report for Kiribati's coral reefs. http://horizon.documentation.ird.fr/exl-doc/pleins_textes/divers14-11/010032214.pdf

Magel JMT, Burns JHR, Gates RD, Baum JK (2019) Effects of bleaching-associated mass coral mortality on reef structural complexity across a gradient of local human disturbance. Sci Rep. https://doi.org/10.1038/s41598-018-37713-1

Ministry of Finance and Economic Development (2016) 2015 Population and Housing Census. Tarawa: National Statistics Office. http://www.mfed.gov.ki/statistics/documents/2015_Population_Census_Report_Volume_1final_211016.pdf

Monismith SG (2007) Hydrodynamics of coral reefs. Annu Rev Fluid Mech 39:37–55

Monismith SG, Rogers JS, Koweek D, Dunbar RB (2015) Frictional wave dissipation on a remarkably rough reef. Geophys Res Lett 42:4063–4071

Oksanen J, Blanchet FG, Friendly M, Kindt R, Legendre P, McGlinn D, Minchin PR, O'Hara RB, Simpson GL, Solymos P, Stevens MHH, Szoecs E, Wagner H (2020) vegan: community ecology package. R package version 2.5–7. https://CRAN.R-project.org/package=vegan

Padilla-Gamiño JL, Hanson KM, Stat M, Gates RD (2012) Phenotypic plasticity of the coral *Porites rus*: Acclimatization responses to a turbid environment. J Exp Mar Biol Ecol 434–435:71–80

Perry CT, Morgan KM (2017) Bleaching drives collapse in reef carbonate budgets and reef growth potential on southern Maldives reefs. Sci Rep. https://doi.org/10.1038/srep40581

Perry CT, Alvarez-Filip L, Graham N, Mumby PJ, Wilson SK, Kench PS, Manzello DP, Morgan KM, Slangen ABA, Thompson DP, Januchowski-Hartley F, Smithers SG, Steneck RS, Carlton R, Edinger EN, Enochs IC, Estrada-Saldívar N, Haywood MDE, Kolodziej G, Murphy GN, Pérez-Cervantes E, Suchley A, Vanlentino L, Boenish R, Wilson M, Macdonald C (2018) Loss of coral reef growth capacity to track future increases in sea level. Nature 558:396–400

Pinheiro J, Bates D, DebRoy S, Sarkar D, R Core Team (2019) nlme: linear and nonlinear mixed effects models. R package version 3.1–140. https://CRAN.R-project.org/package=nlme

Price DM, Robert K, Callaway A, Lo lacono C, Hall RA, Huvenne VAI (2019) Using 3D photogrammetry from ROV video to quantify cold-water coral reef structural complexity and investigate its influence on biodiversity and community assemblage. Coral Reefs 38(5):1007–1021

Principe P, Bradley P, Yee S, Fisher W, Johnson E, Allen P, Campbell D (2012) Quantifying Coral Reef Ecosystem Services. U.S. Environmental Protection Agency, Research Triangle Park

Quataert E, Storlazzi C, van Rooijen A, Cheriton C, van Dongeren A (2015) The influence of coral reefs and climate change on wave-driven flooding of tropical coastlines. Geophys Res Lett 42:5407–6415

R Core Team (2019) R: a language and environment for statistical computing (version 3.5.1). Vienna: R Foundation for Statistical Computing. https://www.R-project.org/

Sappington JM, Longshore KM, Thompson DB (2007) Quantifying landscape ruggedness for animal habitat analysis: a case study using bighorn sheep in the Mojave Desert. J Wildl Manag 71:1419–1426

Sheppard C, Dixon DJ, Gourlay M, Sheppard A, Payet R (2005) Coral mortality increases wave energy reaching shores protected by reef flats: example from the Seychelles. Estuar Coast Shelf Sci 64:223–234

Storlazzi CD, Gingerich SB, van Dongeren A, Cheriton OM, Swarzenski PW, Quataert E, Voss CI, Field DW, Annamalai H, Piniak GA, McCall R (2018) Most atolls will be uninhabitable by the mid-21st century because of sea-level rise exacerbating wave-driven flooding. Sci Adv. https://doi.org/10.1126/sciadv.aap9741

Stuart-Smith RD, Brown CJ, Ceccarelli DM, Edgar GJ (2018) Ecosystem restructuring along the Great Barrier Reef following mass coral bleaching. Nature 7716:92–96

Woodroffe CD (2008) Reef-island topography and the vulnerability of atolls to sea-level rise. Glob Planet Change 62:77–96

Yao Y, Zhang Q, Chen S, Tang Z (2019) Effects of reef morphology variations on wave processes over fringing reefs. Appl Ocean Res 82:52–62